Progress In Electromagnetics Research B, Vol. 2, 177–187, 2008

WIDEBAND 180° PHASE SHIFTER USING MICROSTRIP-CPW-MICROSTRIP TRANSITION

A. A. Eldek

Department of Computer Engineering
Jackson State University
JSU Box 17098, Jackson, MS 39217-0198, USA

Abstract—A microstrip 180° phase shifter obtained by a novel design of Microstrip-to-Coplanar Waveguide (CPW)-to-Microstrip transition is presented. The proposed phase shifter is obtained without changing the layer of the second microstrip line. Via holes are used to transfer the current from the top to the bottom substrate layer and vice versa. The presented phase shifter is operating in a wide bandwidth between 5.5 and 18 GHz, with low insertion loss and reflection coefficients. Because the input and output microstrip lines are on the same layer, the presented phase shifter is suitable for a modified class of feeding networks for phased antenna arrays.

1. INTRODUCTION

Microstrip antennas have been popular for decades because they exhibit a low profile, small size, lightweight, low manufacturing cost, high efficiency, and an easy method of fabrication and installation. Furthermore, they are generally economical to produce since they are readily adaptable to hybrid and monolithic integrated circuits fabrication techniques at radio frequency (RF) and microwave frequencies [1]. Among the present areas that extensively utilize microstrip antennas are phased arrays and spatial power combiners [2]. In these applications, there is a particular interest to obtain an increased operational bandwidth of the array; hence the need for wideband antenna element.

Recently, the Double Dipole and Double Rhombus antennas were presented for ultra wideband phased arrays [3, 4]. The Double Rhombus provides 103% bandwidth as a single element; however, due to the deterioration of its radiation patterns at higher frequencies, the useable bandwidth is only 84%. Therefore, a modified two-element array configuration is used to enhance the radiation patterns at the higher frequencies, and accordingly, increase the useable bandwidth to 95%. In this configuration, the second antenna element is rotated 180°, and consequently a 180° phase shift is introduced numerically at its port. Therefore, a microstrip 180° phase shifter is required to be connected to the odd or even number antenna elements in the phased array system. This phase shifter must have at least the same bandwidth of the antenna. Also, it has to start and end with microstrip lines, to be impeded directly into the array feeding network.

The microstrip 180° phase shifter can be designed by employing transitions between different microstrip feedlines like Microstrip, Coplanar Waveguide (CPW) and Coplanar Stripline (CPS). Researchers have done a lot of effort to design different configurations for the transition from CPW to CPS [5–9], CPS to Microstrip [10, 11], CPW to Microstrip [11–13], Probe to Microstrip [14], CPW to slotline [15], parallel striplines to microstrip [16], and conductor backed CPW (CBCPW) to microstrip with a 180° phase shift [17].

In this paper, we present a microstrip 180° phase shifter with ultra wide bandwidth to cover the operating band of the Double Rhombus antenna in [4]. For this phase shifter to be integrated into the feeding network of this antenna array we used the same kind of substrate with the same height, and the input and output microstrip lines must be in the same layer. We employed a Microstrip-to-CPW-to-Microstrip transition and via holes to transfer the current from the top to the bottom substrate layer and vice versa. The presented phase shifter is operating in a wide bandwidth between 5.5 and 18 GHz, with low insertion loss and reflection coefficients. Because the input and output microstrip lines are on the same layer, the presented phase shifter is suitable for a modified class of feeding networks for phased antenna arrays.

The simulation and analysis for the presented phase shifter are performed using the commercial computer software package Ansoft High Frequency Structure Simulator (HFSS) [18], which is based on the finite element method. Measurements of the return loss and transmission coefficient are also conducted for verification of the simulation results.

2. PHASE SHIFTER GEOMETRY

The operation of the proposed microstrip phase shifter is demonstrated in Fig. 1 for infinitesimal transmission lines. The 180° phase shift at the second port is realized by connecting the +ve terminal of port 1 to the −ve terminal of port 2 and vice versa. The phase shifter

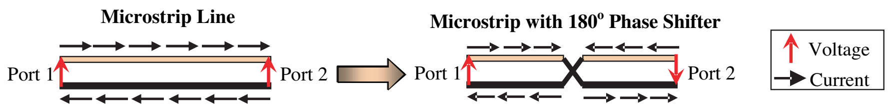

Figure 1. Phase shifter operation.

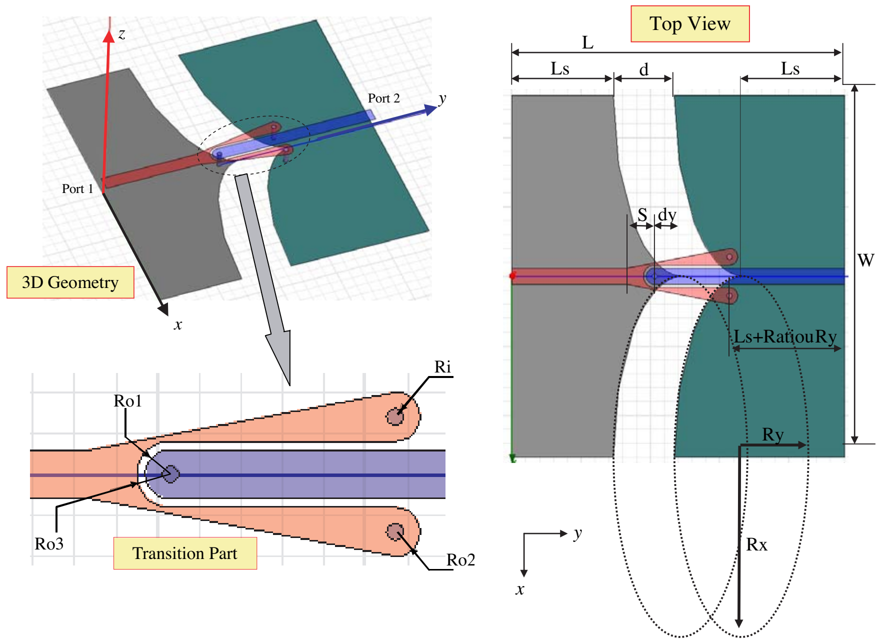

Figure 2. Geometry and parameters of the proposed 180° phase shifter.

is printed on a Rogers RT/Duroid 6010/6010 LM substrate with a dielectric constant of 10.2, a conductor loss ($\tan\delta$) of 0.0023 and a thickness of 25 mil (0.635 mm). The detailed geometry and parameters are illustrated in Fig. 2. Many parameters are introduced in the proposed design which may add more complexity to the design but they give us more flexibility to enhance its characteristics to match different design requirements.

According to Fig. 2, the phase shifter starts and ends with 50Ω microstrip feedlines, of width $= 2\,R_{o1}$, in the upper substrate layer. In the middle, the first microstrip is divided gradually into two branches which surround the second microstrip line to compose a CPW. Then, they are truncated with circles which are concentric with the PEC via holes that connect these ends to the ground plane of the second microstrip. The inner end of the second microstrip line is also circle which is concentric with the PEC via hole that connects this end to the ground plane of the first microstrip. The positions of these circles and their radii, R_{o1}, R_{o2}, R_{o3}, and R_i, are depicted in Fig. 2-Transition Part. In addition, the phase shifter has L: the y-dimension of the shifter, W: the x-dimension of the shifter, L_s: length of the first and second microstrip sections, d: the y-distance between the two ground planes which are defined by four identical ellipses with radii R_x and R_y, S: the distance between the starting point of branching the first microstrip and the center of the via, d_y: the distance between the center of the left via and left ellipse, and Ratio: the parameter that controls the distance between the two right vias and the center of the right ellipse.

This design depends on a smooth transition between the different feedlines. Consequently, it decreases the reflections due to the transmission from certain mode to another. The two branches from the first microstrip start with 100Ω line to match the microstrip, then their width increases gradually to form a ground plane to the CPW. The circles are used to reduce reflections from the vias. The four ellipses provide a tapered cut in the ground planes, concentration of the current close to the vias, and direction of the current from port 1 to port 2.

3. PARAMETRIC ANALYSIS

The design process passed through different stages. Several geometries were proposed until we came up with the one in Fig. 2. Then we studied the effect of each parameter to improve the characteristics of the phase shifter. One parameter is changed at a time, while the other parameters are kept as in Table 1. The dimensions are given in Table 1 in mm except "Ratio" which is dimensionless. Additionally, $R_x = W/2$, and $L_s = (L - d - R_y)/2$. R_{o1} did not change to keep the input impedance 50Ω at the ports. Fig. 3 shows the effect of d. By decreasing d, we can increase the bandwidth with trade between the return loss level and the bandwidth. The best transmission coefficient is at $d = 2$ mm. Next, Fig. 4 shows the effect of d_y. This distance is a matching stub to the transition between the first microstrip and the CPW.

Table 1. Phase shifter dimensions in mm.

W	L	Ry	d	Ri	Ro1	Ro2	Ro3	S	dy	Ratio
13	12	2.5	2.2	0.1	0.3	0.3	0.4	1	1	0.2

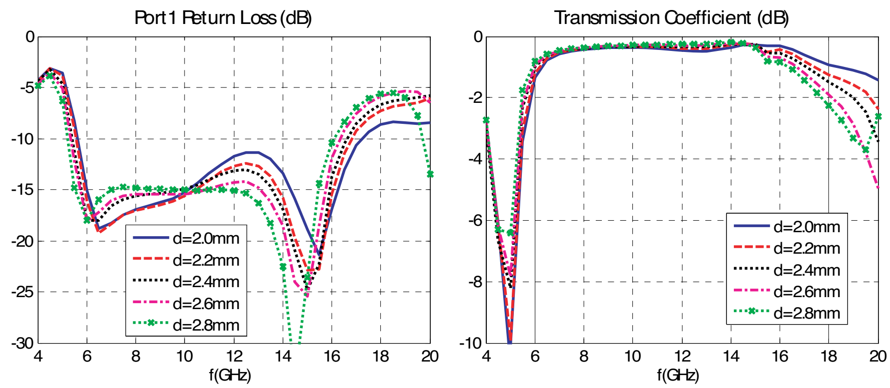

Figure 3. Effect of d on the return loss and transmission coefficient.

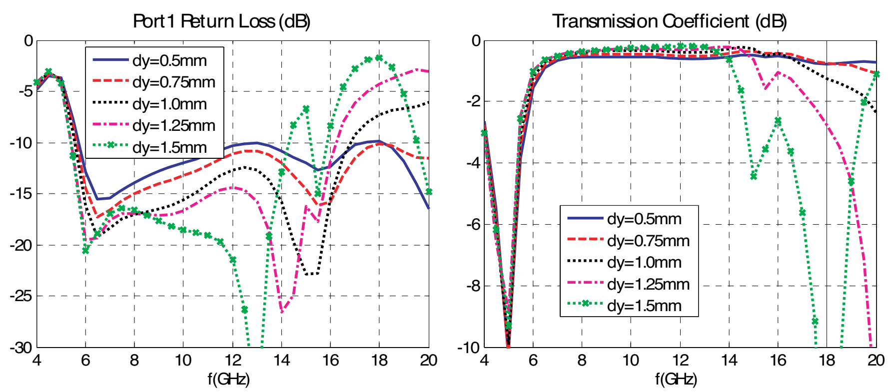

Figure 4. Effect of d_y on the return loss and transmission coefficient.

The best bandwidth and transmission is obtained at $d = 0.75$ mm, where the phase shifter operates from 5.7 to more than 20 GHz. Fig. 5 demonstrates the effect of Ratio, which controls the matching between the CPW and the second microstrip. The best results are obtained at Ratio $= 0.2$. Fig. 6 shows the effect of R_i, which changes the impedance of the via. The best results are obtained when $R_i = 0.2$ mm. The effect of R_{o2} is shown in Fig. 7. It has a small effect compare to the effect of R_{o3}, which is shown in Fig. 8. By increasing R_{o3} we are able to improve both return loss and transmission with some decrease in the bandwidth. The effect of R_y, as shown in Fig. 9, is opposite to that of R_{o3}. As R_y increases the bandwidth increases, but both return loss and transmission deteriorate. The effect of the last parameter, S, is

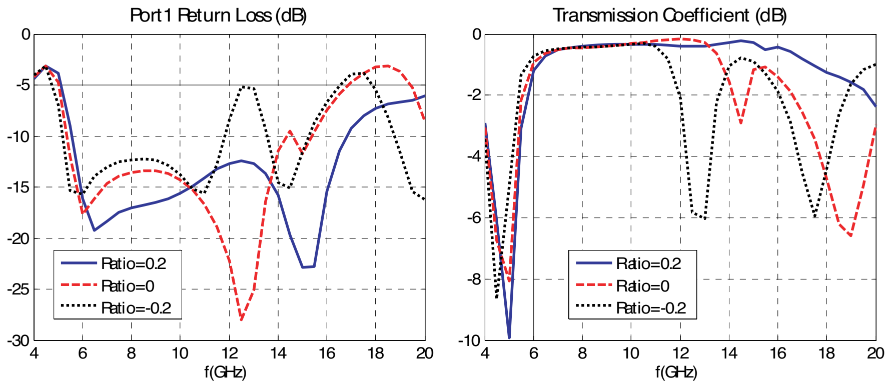

Figure 5. Effect of ratio on the return loss and transmission coefficient.

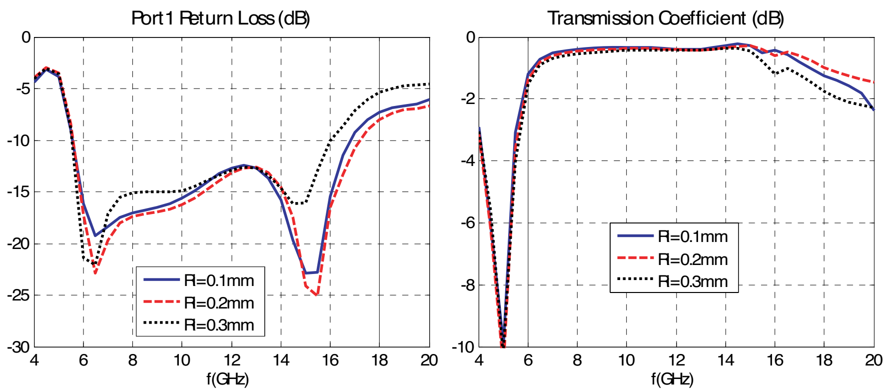

Figure 6. Effect of R_i on the return loss and transmission coefficient.

shown in Fig. 10. It can be tuned to improve the return loss.

In order to verify the computed results using HFSS, the prototype shown in Fig. 11, was fabricated using milling machine with the dimensions in Table 1, and measured using Agilent E5071B Network Analyzer (ENA Series) in the Oak Ridge National Laboratory. The measured and computed return loss and transmission coefficient are depicted in Fig. 12, with a quite good matching between the two results. The phase shifter operates from 5.5 to 17.2 GHz with an approximate average return loss of -15 dB and transmission coefficient of -0.4 dB in this frequency range. Finally, the transmission coefficient of a microstrip line whose length is $L + 0.635$ mm is simulated and measured. The 0.635 mm (via height) is added to substitute for

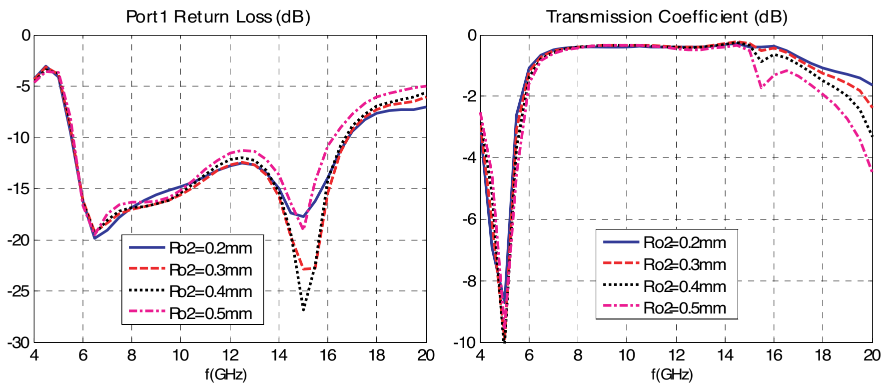

Figure 7. Effect of R_{o2} on the return loss and transmission coefficient.

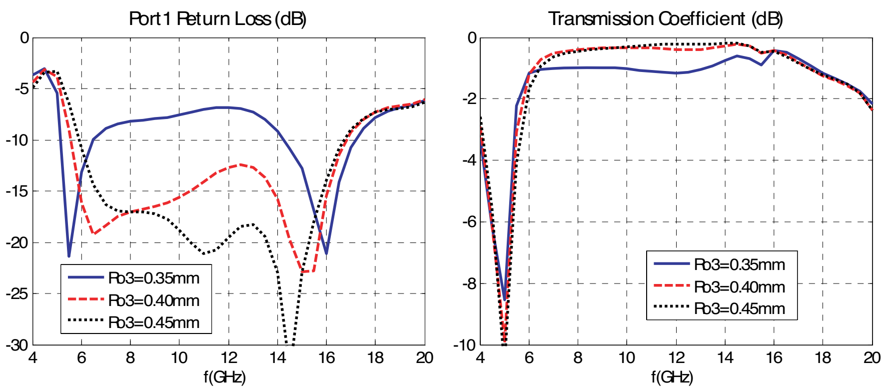

Figure 8. Effect of R_{o3} on the return loss and transmission coefficient.

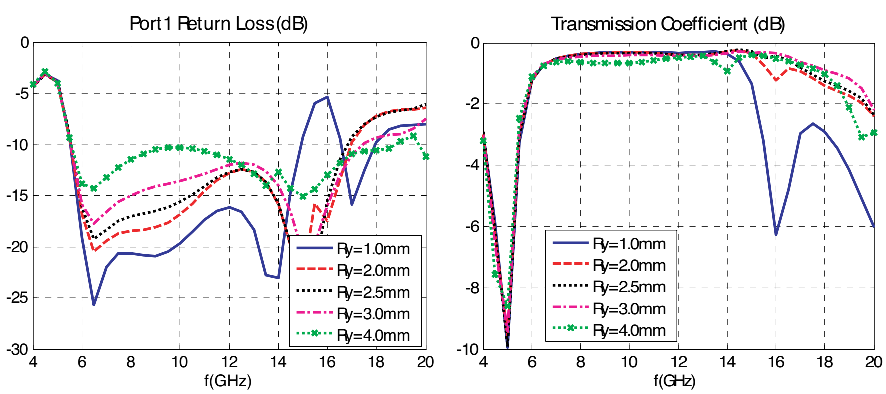

Figure 9. Effect of R_y on the return loss and transmission coefficient.

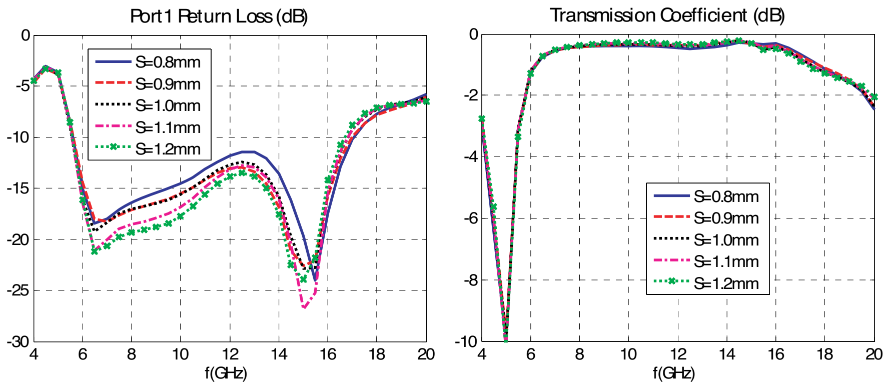

Figure 10. Effect of S on the return loss and transmission coefficient.

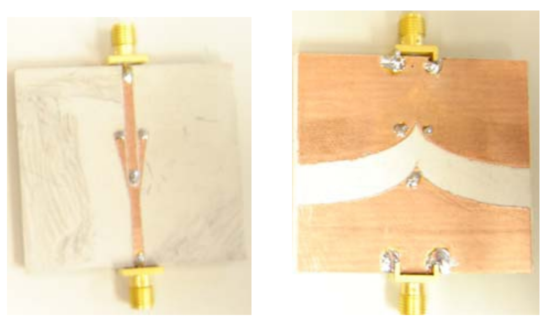

Figure 11. Prototype of the proposed phase shifter: Top view (left), and back view (right).

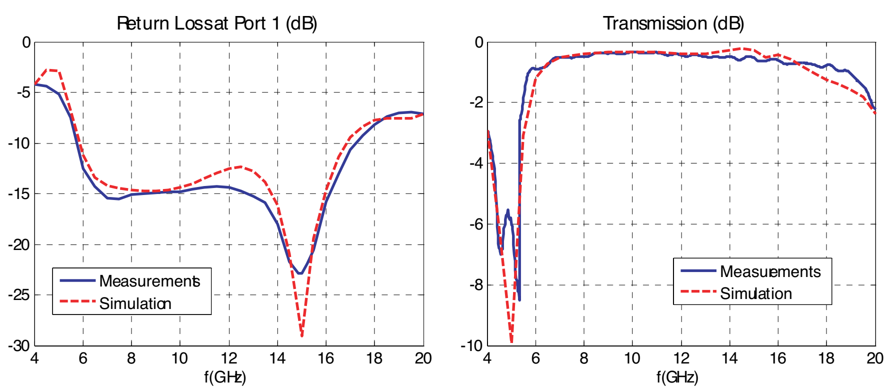

Figure 12. Measured and computed results.

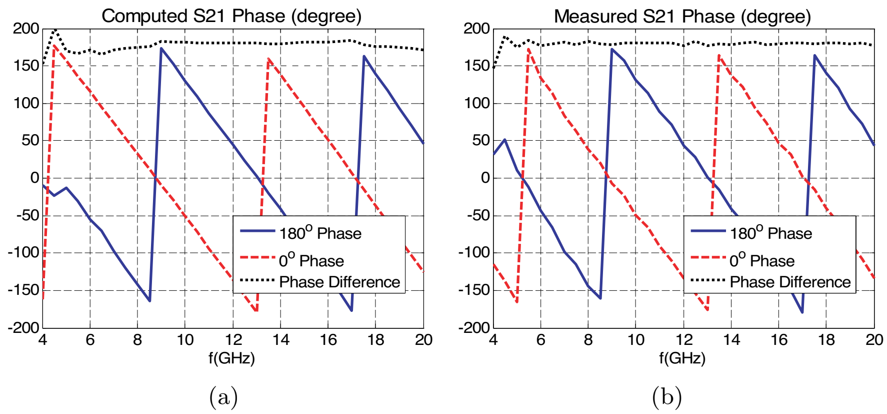

Figure 13. S_{21} phase shift in degrees: (a) Computed results, and (b) Measured results.

extra current path through the vias. The measured and computed transmission coefficient phases in degrees are shown in Fig. 13 for the 180° phase shifter and the microstrip line. In both graphs of Fig. 13, the dotted line, which is the absolute difference between the two phases, shows that an approximate phase difference of 180° is obtained between 5 and 20 GHz.

4. CONCLUSIONS

The proposed 180° phase shifter can be directly integrated in the feeding network of the Double Rhombus antenna array because it is composed form the same material and its input and output ports are in the same layer. The results show that it can operate in a wide frequency band from 5.5 to more than 20 GHz with high transmission coefficient and an approximate phase shift of 180° in the entire operating range. By integrating this phase shifter with the Double Rhombus we can definitely improve its radiation characteristics and increase its usable bandwidth in phased arrays and power combiners.

ACKNOWLEDGMENT

The author would like to thank the RF and Microwave group of the Oak Ridge National Laboratory, Oak Ridge, TN, for their great support and help in building and measuring the proposed design in this paper.

REFERENCES

1. Maloratsky, L. G., "Reviewing the basics of microstrip lines," *Microwave & RF*, 79–88, March 2000.
2. Mailloux, R. J., *Phased Array Handbook*, Artech House, Boston, 1994.
3. Eldek, A. A., "Design of double dipole antenna with enhanced usable bandwidth for wideband phased array applications," *Progress In Electromagnetics Research*, PIER 59, 1–15, 2006.
4. Eldek, A. A., "Ultra wideband double rhombus antenna with stable radiation patterns for phased array applications," *IEEE Trans. Antennas Propagat.*, Vol. 55, No. 1, 84–91, Jan. 2007.
5. Kim, S., S. Jeong, Y. T. Lee, D. H. Kim, J. S. Lim, K. S. Seo, and S. Nam, "Ultra-wideband (from DC to 110 GHz) CPW to CPS transition," *Electronic Lett.*, Vol. 38, No. 13, 622–623, Jun. 2002.
6. Tilley, K., X. D. Wu, and K. Chang, "Wideband transition from conductor-backed coplanar waveguide to modified coplanar stripline using multiple substrates," *Electronic Lett.*, Vol. 29, No. 23, 2051–2052, Nov. 1993.
7. Ho, C. H., L. Fan, and K. Chang, "Broad-band uniplanar hybrid-ring and branch-line couplers," *IEEE Trans. Microwave Theory and Techniques*, Vol. 41, No. 12, 2116–2125, Dec. 1993.
8. Prieto, D., J. C. Cayrou, J. L. Cazaux, T. Parra, and J. Graffeul, "CPS structure potentialities for MMICs: a CPS/CPW transition and a bias network," *IEEE MTT-S International Microwave Symposium Digest 1998, Baltimore, MD*, Vol. 1, 111–114, Jun. 1998.
9. Mao, S. G., C. T. Hwang, R. B. Wu, and C. H. Chen, "Analysis of coplanar waveguide-to-coplanar stripline transitions," *IEEE Trans. Microwave Theory and Techniques*, Vol. 48, No. 1, 23–29, Jan. 2000.
10. Suh, Y.-H. and K. Chang, "A wideband coplanar stripline to microstrip transition," *IEEE Microwave and Wireless Components Lett.*, Vol. 11, No. 1, 28–29, Jan. 2001.
11. Safwat, A. M. E., K. A. Zaki, W. Johnson, and C. H. Lee, "Novel transition between different configurations of planar transmission lines," *IEEE Microwave and Wireless Components Letters*, Vol. 12, No. 4, 128–131, Apr. 2002.
12. Zheng, G., J. Papapolymerou, and M. M. Tentzeris, "Wideband coplanar waveguide RF probe pad to microstrip transitions without via holes," *IEEE Microwave and Wireless Components Letters*, Vol. 13, No. 12, 544–546, Dec. 2003.

13. Maya, M. C., A. Lazaro, P. DePaco, and L. Pradell, "A method for characterizing coplanar waveguide-to-microstrip transitions, and its of microstrip devices with coplanar microprobes," *Microwave Optical Tech. Lett.*, Vol. 39, No. 5, 373–378, Dec. 2003.
14. Reiche, E. and F. H. Uhlmann, "Application of the FDTD for the optimization of broad-band transitions between different types of transmission lines," *IEEE Trans. On Magnetics*, Vol. 38, No. 2, 593–596, Mar. 2002.
15. Oldenburg, M. K. and T. M. Weller, "High-efficency CPW-to-slotline transitions on low ε_r substrates," *Microwave Optical Tech. Lett.*, Vol. 41, No. 2, 91–93, Apr. 2004.
16. Abbosh, A. M. and M. E. Bialkowski, "An UWB planar out-of-phase power divider employing parallel stripline-microstrip transitions," *Microwave Optical Tech. Lett.*, Vol. 49, No. 4, 912–914, Apr. 2007.
17. Mousavi, P., R. R. Mansour, and M. Daneshmand, "A novel wide band 180-degree phase shift transition on multilayer substrates," *IEEE MTT-S International Microwave Symposium Digest 2004*, 1887–1890, Jun. 2004.
18. HFSS: High Frequency Structure Simulator Based on the Finite Element Method, ver. 10, Ansoft Corp., 2005.